Langmuir

Article

pubs.acs.org/Langmuir

Vibrational Modes of Elongated Sessile Liquid Droplets

Robert H. Temperton and James S. Sharp*

School of Physics and Astronomy and Nottingham Nanotechnology and Nanoscience Centre, University of Nottingham, Nottingham NG7 2RD, United Kingdom

Supporting Information

ABSTRACT: Vibrations of small (microliter) sessile liquid droplets were studied using a simple optical deflection technique. The droplets were made to elongate in one direction by taking advantage of the anisotropic wetting of the liquids on structured diffraction grating surfaces. They were vibrated by applying a puff of nitrogen gas. Motion of the droplets was monitored by scattering laser light from their surfaces. The scattered light was collected using a photodiode, and the resulting time-dependent intensity signals were Fourier-transformed to obtain the vibrational response of the drops. The vibrational spectra of elongated sessile drops were observed to contain two closely spaced peaks. A simple model that considers the frequency of capillary wave fluctuations on the surfaces of the drops was used to show that the vibrational frequencies of these peaks correspond to standing wave states that exist along the major and minor profile lengths of the droplets.

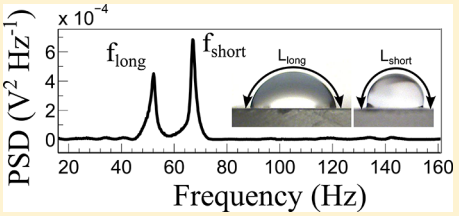

INTRODUCTION

The influence of wetting phenomena and drop shape on the vibrational response of small (microliter) droplets is key to understanding how they move on chemically and topographically patterned substrates.[1−6] Vibrations applied to the droplets allow them to undergo large-amplitude shape oscillations at their mechanical vibrational frequencies and, thus, to sample nearby shape configurations. In this way, the drops are able to move to areas of lower interfacial energy on the substrate, and a net force is created that drives the unidirectional motion of the drops along wettability gradients. The potential for application of this technique to drive the motion of droplets in microfluidic systems has generated a renewed interest in the physics of droplet vibration.[2,3] However, the frequency of droplet oscillations has been observed to depend upon the amplitude of the vibration when large perturbations are applied to the droplets,[7−9] and a greater understanding of how these frequency-dependent amplitude fluctuations drive droplet motion is still required.

Droplet vibration is also important in processes such as droplet atomization, in which a small amount of liquid is placed on a surface or emitted from a nozzle and vibrated in such a way that its resonant modes are excited.[10] When higher order (short wavelength) modes are excited with sufficiently large amplitudes, the vibrations can result in ejection of material from the droplet.[11] This phenomenon has found application in areas such as inkjet printing, fuel injection, spray coating, nebulization,[12] and electrospray deposition,[13] where the production of droplets with a well-defined size distribution is required. Droplet vibration has also recently been used to control the small-scale mixing/demixing of fluids[14] and as a tool for measuring the surface tension[15−17] and viscosity[18] of sessile and levitated drops. In addition, models based on liquid droplet vibrations have also been used in attempts to describe the properties of neutron stars[19] and atomic nuclei.[20] Moreover, there is an increasing interest in the general phenomenon of liquid wetting/spreading at an interface,[21−23] including contact angle hysteresis effects[24] and anisotropic wetting phenomena.[25,26]

Various attempts have been made to measure the vibrational response of sessile droplets by direct visualization of the droplet modes using high-speed cameras[11,27] and also using optical-deflection-based techniques.[16,18] Droplet oscillations can be driven using direct mechanical vibration at fixed frequencies,[11,27,28] by applying a mechanical impulse to the drops[16,18] or using electromagnetic fields.[29] Recent experiments have also used white noise to excite the vibrations of small liquid drops.[30]

The first theory of drop vibration was developed for free/unsupported droplets by Rayleigh.[31] He showed that the vibrational frequencies of droplets are determined by their mass/size and the surface tension of the liquid. This theory was later extended by Lamb[32] and Chandrasekhar[33] to include the effects of viscous damping. These authors showed that the width of the droplet mechanical resonances are determined by the viscosity and density of the liquid as well as the drop size. Theories of vibration in sessile droplets have also been developed by numerous authors.[28,34−41] However, the most intuitive of these approaches involves a relatively simplistic approximation that was developed by Noblin and co-workers.[28] These authors suggested that the resonant vibrational states of drops with pinned contact lines could be described by assuming that a half integer number of vibrational wavelengths, λ, fit along the profile length, L, of the drops; i.e., $n\lambda/2 = L$, where n is the mode number (see Figure 1). When this condition is combined with the expression for the dispersion properties of capillary−gravity waves on the surface of a liquid bath,[42] it gives

Received: November 13, 2012
Revised: March 19, 2013
Published: March 21, 2013

   dx.doi.org/10.1021/la304520c | Langmuir 2013, 29, 4737−4742

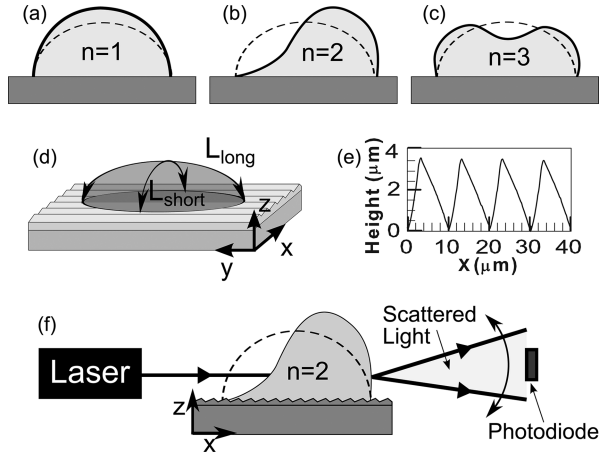

Figure 1. Drop shapes and experimental setup. (a, b, and c) Diagrams showing the expected shapes of the n = 1, 2, and 3 modes of a vibrating sessile droplet, respectively. The n = 1 mode requires a change in volume when the contact line remains pinned. In this case, the lowest allowed mode for an incompressible liquid is the n = 2 mode. (d) Schematic showing the geometry of a droplet placed on a surface patterned with horizontal grooves. The diagram illustrates how the long and short profile lengths, L_{short} and L_{long}, of such an aspherical droplet are defined. (e) AFM line profile of the ruled diffraction grating used in this study. (f) Schematic of the experimental setup used to measure the droplet vibrations. A helium−neon laser light was scattered off the droplets. Oscillations (such as the n = 2 mode shown) were excited by applying an impulse in the form of a short puff of nitrogen gas. These oscillations were detected using a photodiode to measure fluctuations in the scattered light intensity.

an expression for the vibrational frequency, f, of the droplets. In the limit where the droplets are smaller than the capillary length of the fluid [$l_{cap} = (\gamma/\rho g)^{1/2} \sim 2.7$ mm for water], we obtain

$$f = \sqrt{\frac{n^3\pi\gamma}{4\rho L^3}\tanh\left(\frac{n\pi h}{L}\right)} \quad (1)$$

where γ and ρ are the surface tension and density of the liquid, respectively, h is the average height of the droplet,[28] and g is the acceleration due to gravity. This result was shown to agree well with experiments[28] and was later confirmed by Sharp et al.,[16] who used a modified version of this theory to derive an expression for the contact angle dependence of the resonant frequencies of sessile drops. The mode number, n, describes the number of half wavelengths that fit along the meridonal profile of the sessile drop and can assume integer values of n = 2, 3, 4, ... Previous work by Sharp et al.[16,18] has confirmed that n = 2 corresponds to the lowest vibrational mode, which conserves volume for sessile drops when the contact line remains pinned. The results of these studies and the drop shapes expected for the n = 2 mode were also found to be in agreement with the frequencies and drop shapes reported by Daniel et al.,[6] who described the lowest frequency (fundamental) mode in terms of a "rocking" motion. Examples of the drop shapes expected for the different modes are shown in panels a−c of Figure 1. In the case where the contact line remains pinned, it acts as a vibrational node. In the n = 1 case, only one-half of a wavelength exists along the profile length of the drop, and hence, a single antinode would be present on the surface of the drop (see Figure 1a). This type of motion requires a change in volume of the drop and is therefore forbidden for an incompressible fluid. This constraint is likely to be relaxed in cases where the contact line becomes unpinned during vibration. In such a case, a single vibrational node would exist on the surface of the drop and two antinodes would occur at the contact line. The n = 1 mode would therefore conserve volume and be allowed.

The above model of sessile drop vibration assumes that a microliter liquid droplet with a radius of curvature less than the capillary length of the fluid will form a spherical cap when placed on a surface. The actual shape of the droplet is then determined by the three-phase contact angle subtended at the liquid/substrate/air interface.[43] However, inhomogeneities in the surface properties of substrates and the presence of contact angle hysteresis effects[44] can lead to spatial variations in the three-phase contact angle. As a result, a distribution of profile lengths, L, may exist, giving rise to a range of different vibrational frequencies. Previous studies have shown that this variation in contact angle can be eliminated to some extent by vibrating the droplets with large amplitudes in such a way as to allow for the three-phase contact line to sample nearby configurations and to obtain a contact angle close to the equilibrium value for the surface and liquid being studied.[27,45]

In the case of structured and gradient surfaces, where wettability of microliter liquid droplets is controlled by varying either the local chemical[46] or topographic[1] structure of the surface, vibration of the droplets does not result in a uniform contact angle. Anisotropy gives rise to spatial and/or orientational differences in the wetting properties of these substrates depending upon the chemical and physical structures that are present. This is particularly true in the case where surfaces are patterned with anisotropic topographic features. For example, droplets that are deposited on surfaces that have been patterned with periodic grooves have been shown to display strongly anisotropic wetting properties.[25,26]

Here, we study the vibrational properties of microliter liquid droplets on the surface of corrugated substrates. We show that the anisotropic wetting of the drops causes a splitting of the fundamental mode of droplet vibration and that the two closely spaced vibrational frequencies correspond to standing wave states that exist along the profile lengths corresponding to the major and minor drop axes. The results presented are important for understanding the vibrational behavior of drops on surfaces with anisotropic wetting properties, such as those that have been used to drive droplet motion. The vibrational-based approach that is discussed below also has potential applications in the study of anisotropic wetting phenomena and contact line pinning effects.

■ EXPERIMENTAL SECTION

Microliter volume water droplets were deposited on the surface of an aluminum, blazed, ruled diffraction grating (ThorLabs, GR1325-10106) using a micropipet. A typical line profile taken from an image of one of the substrates used was obtained using an Asylum Research MFP-3D atomic force microscope (AFM) and is illustrated in Figure 1. Droplets placed on these surfaces were observed to spread anisotropically until they formed elongated liquid caps whose major and minor basal axes lay parallel and perpendicular to the axis of the grooves, respectively (see Figure 1d).

Vibration was induced in the droplets by applying an impulse in the form a small puff of nitrogen gas. The puff was delivered through a sintered brass diffuser attached to the end of an 8 mm diameter plastic tube placed ∼5 cm above the droplets. The duration of the pulse was controlled using an electrically actuated pneumatic valve and was maintained for ∼0.1 s for all of the experiments performed in this work.

dx.doi.org/10.1021/la304520c | Langmuir 2013, 29, 4737−4742

The vibrations were monitored using a simple technique, where a He−Ne (633 nm) laser with a beam diameter of 0.8 mm was passed through the droplet and refracted at the drop interfaces (see Figure 1f). The droplets acted like a poor-quality lens, producing a cone of scattered light, which, when captured on a screen or detector, produced a slightly elliptical spot with a radial gradient in intensity. Changes in the shape of the droplet during vibration caused the refraction angle of the scattered light cone to change with time. Time-dependent variations in the intensity of laser light scattered by the drops were measured using a photodiode (RS Components, U.K.) connected to a home-built amplifier circuit and a USB data acquisition card (National Instruments, USB-6008). As the droplets vibrated and the cone of scattered light moved, the radial intensity gradients present in the scattered beam gave rise to variations in the electrical signal measured by the photodetector. In this way, variations in intensity could be used to provide information about the motion of the drop. These time-dependent signals were then Fourier-transformed to obtain the vibrational spectra of the droplets. For each impulse, 5 s of data was recorded at 1000 Hz, giving a resolution in the power spectrum of 0.2 Hz. Each measurement was repeated 2−3 times to ensure that the vibrational frequencies of the drops were reproducible and the shape of the drops did not change during vibration. The mass of the droplets was also measured both before and after vibration using an analytical balance (Fisher Scientific, PS-200) to ensure that significant evaporation losses did not occur. No discernible changes were observed in the measured vibrational frequencies and shapes of the drops during an individual measurement, and no change in the mass of the drops was observed within the limits of experimental uncertainty (±0.0001 g). Each individual measurement (plus repeats) took less than 2 min to collect. This short experimental time scale was used to ensure that considerable contamination of the water surface did not occur during the experiments. Previous studies[11] have considered the time scales associated with contamination of a free water surface in air and have shown that significant contamination occurs on time scales of ∼5 min.

Images of the drops were obtained along their major and minor axes using a Philips SPC100NC webcam (see inset of Figure 2). These images were used to determine the profile lengths and average height of the droplets. A Genie HC640 camera (Teledyne DALSA, 200 frames per second) was also used to obtain movies of the vibrating droplets to allow for comparison of the observed and expected droplet shapes during vibration and to monitor the motion of the contact line during vibration (see the Supporting Information). In all cases, the three-phase contact line was observed to remain pinned during the experiments.

RESULTS AND DISCUSSION

An example of the time-dependent light scattering data collected for a 5 μL droplet is shown in Figure 2. This droplet was observed to spread in such a way that gave basal radii of 1.6/1.1 mm and profile lengths of 4.8/4.1 mm along the major/minor axis of the drop. The Fourier transform of the time-dependent intensity data for this drop is shown in the middle panel of Figure 2. It clearly shows that there are two distinct but closely spaced vibrational peaks at 52.4 ± 0.2 and 67.2 ± 0.2 Hz. A spherical cap droplet of a similar size and comparable profile length would be expected to display a single vibrational peak in this region (examples are shown in Figure 2c.

The observation of peak splitting reported here (and shown in Figure 2b) is consistent with studies of levitated droplets, where it has been shown that small deviations from sphericity result in the splitting of the resonant modes.[47] Three distinct but closely spaced vibrational modes are typically observed in ellipsoidal levitated drops, which correspond to surface vibrations along the principal axes of the ellipsoid. In elongated sessile drops, one of these modes is suppressed because it would require vibration and displacement of fluid around the

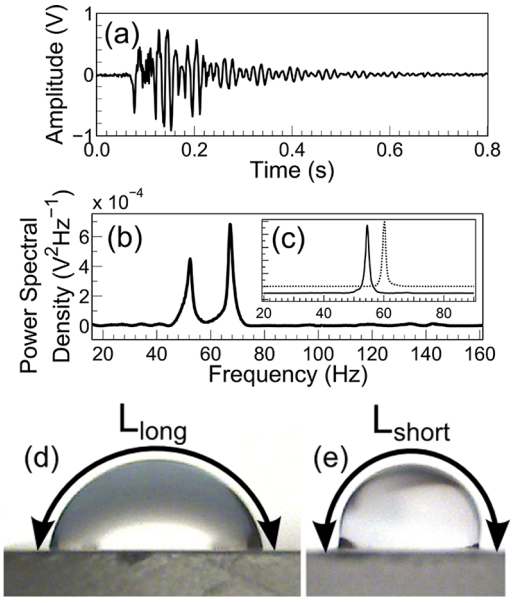

Figure 2. Example data set obtained for a 5 μL droplet placed on a blazed diffraction grating. (a) Time-dependent variations in the photodiode voltage measured when the drop was perturbed by a short puff of nitrogen gas. Fourier transformation of the time-dependent data in panel a gives the power spectra shown in panel b. The peaks at higher and lower frequencies correspond to surface waves that exist along the short and long droplet profiles, respectively. Equivalent spectra for two different spherical cap water droplets on a polydimethylsiloxane (PDMS) substrate are shown in panel c. These droplets have similar profile length values (4.6 mm, solid line; 4.2 mm, dashed line) to the long and short axes (4.8 and 4.1 mm, respectively) of the elongated drop studied in panels a and b. These plots are offset along the vertical axis to enable comparison. Panels d and e show photographs of the long and short profile lengths of the drop studied in panels a and b.

boundary defined by the three-phase contact line. Motion of the contact line did not occur in our experiments. This was confirmed by the observation that the contact line remained pinned during vibration.

Figure 3 shows how the relative amplitudes of the two vibrational peaks observed in elongated sessile drops vary as the major axis of the drop is rotated in the plane of the sample. In these experiments, the major axis was rotated by an angle α relative to the direction of propagation (plane of incidence) of the incident laser beam (see panels a−c of Figure 3 for examples of how α is defined). The plot in Figure 3 shows that the ratio of the amplitudes of the two peaks is dependent upon the orientation of the drop axes relative to the laser beam and that the frequencies of the two peaks remain approximately constant. The frequencies of both peaks were found to increase only very slightly with time (corresponding to an increasing angle of rotation; see bottom panels of Figure 3) because of evaporation from the droplet surfaces during these extended experiments.

Figure 3 also shows that, when the one of the principal axes of the drop is parallel to the incident laser beam (corresponding to $\alpha = 90°$), only one of the two peaks is observed. As the droplet was rotated, the ratio of the amplitudes was observed to vary monotonically from a situation where one peak was dominant in the spectrum to one where the other peak dominated. The measurement geometry was such that the peak associated with the major axis was dominant when the plane of

dx.doi.org/10.1021/la304520c | Langmuir 2013, 29, 4737−4742

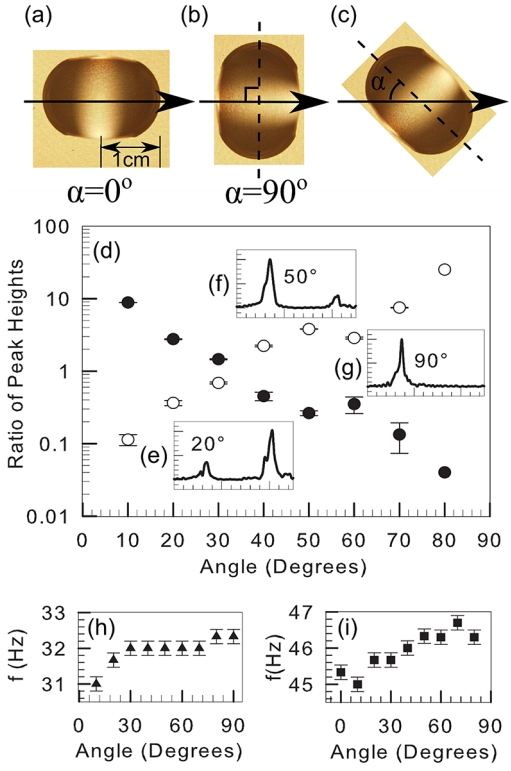

Figure 3. Effects of rotating elongated droplets. Panels a–c show how the angle of rotation α is defined (see the text). The arrows represent the direction of propagation of the laser beam, and the dashed line marks the long axis of the drop (also the groove axis on the substrate). The main panel, d, shows the mean ratio of the two peak heights plotted as a function of the angle (α) for a 15 μL drop. This was repeated 3 times for the same drop. The solid symbols show the ratio of the amplitudes of the high-frequency peak to the low-frequency peak, and the hollow symbols show the inverse of this ratio. Panels e, f, and g show examples of normalized spectra obtained from the first repeat that were collected at values of α = 20°, 50°, and 90°, respectively. Panels h and i show how the position of the low- and high-frequency peaks shifted during the first repeat, respectively. The increase in frequency as the angle increases is the effect of evaporation decreasing the drop volume. The further two repeats showed comparable evaporation rates.

incidence was parallel to the minor axis of the droplet and vice versa. These combined observations support the idea that the peaks correspond to vibrations along the profile lengths corresponding to the major and minor axes of the drops. If this is the case, then an approach similar to that adopted by Noblin et al. can be applied to try to predict the frequencies of the peaks in the vibrational spectra of elongated sessile liquid drops. A simple analysis can be used on the basis of eq 1, where the single profile length, L, is replaced with the two profile lengths corresponding to the major and minor axes (L_{long} and L_{short}).

Figure 4 shows how the square of the frequencies of the individual peaks vary as a function of the product L_i^{-3} $\tanh(n_i\pi h/L_i)$ (where i = short or long) for elongated sessile drops with volumes in the range of 3–20 μL, supported on corrugated diffraction grating surfaces. In each case, measurements were performed at values of θ = 0° and 90°. Photographs of the drops were used to extract their long and short profile lengths and to determine the average drop heights.

According to eq 1, all of the data shown in Figure 4 should collapse on to a single straight line, whose gradient depends

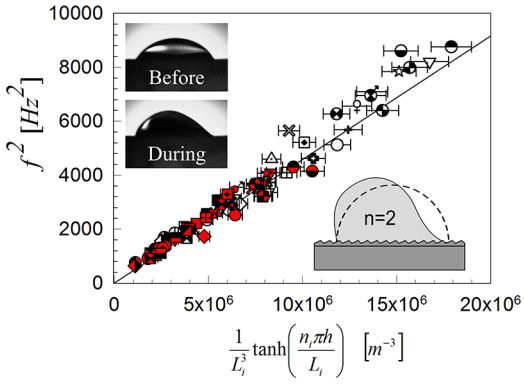

Figure 4. Plot showing the square of the frequency of the fundamental mode of vibration, f^2, as a function of L_i^{-3} $\tanh(n_i\pi h/L_i)$, where i = long or short. As predicted, the frequencies corresponding to the long (filled symbols) and short (hollow symbols) profile lengths collapse on to a single line. Different symbols are used for each individual droplet. The solid line was generated from eq 1 using values of γ = 72.8 mJ m^{-2}, ρ = 998 kg m^{-3}, and n_{short} = n_{long} = 2. The insets show the predicted shape of the n = 2 mode and the actual shape of a 20 μL drop before and during vibration (viewed along the long axis of the drop).

upon the surface tension and density of the liquid and the mode number, n_i. Figure 4 shows that the data does indeed collapse in this way. The solid line in Figure 4 was generated using eq 1, with values of γ = 72.8 mJ m^{-2} and ρ = 998 kg m^{-3} for water[48] Values of n_{long} = n_{short} = 2 were used because these are expected to correspond to the lowest vibrational mode that conserves volume in elongated sessile droplets. However, we note that, for higher frequency modes, there is no reason why the mode numbers for the long and short axes should be the same. In fact, providing that volume is conserved and the boundary conditions for the displacement at the very top of the drop are matched, higher modes would be expected to assume different combinations of n_{short} and n_{long}. A comparison of an image obtained using the Genie HC640 camera and the expected drop shapes for the lowest frequency mode of the elongated drops is shown in Figure 4 and was found to be in good agreement. We note that the shape of the fundamental mode of the drops shown in this figure is similar to that reported for spherical cap drops reported by Sharp[18] and Daniel et al.[6]

The average height of the droplets, h, was calculated numerically. This was performed by fitting ellipses to the profiles extracted from photographs of the drops. These fits were then used to reconstruct the shape of the droplet by assuming that they had an ellipsoidal shape. An estimate of the height of the elongated drops was then obtained at different positions on its surface, and these were used to calculate a value of h. The ellipsoidal cap approximation was found to reproduce the volume of the drop to within 10% of the true measured values. In each case, the mass/volume of the drop was determined by carefully weighing the substrates before and after the drops were deposited. The approximation used here gave rise to uncertainties of ~3–4% in the average drop heights. This approximation was the dominant source of uncertainty in these experiments and gives horizontal error bars of ~5–7% in Figure 4.

The fact that all of the data can be described by a modified version of eq 1 using literature values of the surface tension and density of water is extremely encouraging. Moreover, the

dx.doi.org/10.1021/la304520c | Langmuir 2013, 29, 4737–4742

agreement with the predicted scaling of the frequency with the profile lengths of the major and minor axes of the drops provides extremely strong evidence that the existence of standing wave states along the principal axes give rise to the peaks in the vibrational spectra of elongated liquid droplets.

CONCLUSION

We have shown that asymmetry in the shape of microliter sessile liquid droplets gives rise to a splitting of their vibrational modes. A simple theory of droplet vibration can be used to relate the shape of the drops to the measured frequencies of vibration. The experimental approach adopted in this work is extremely simple to implement. These combined experiments show that it is possible to predict the vibrational frequencies of droplets on topographically structured surfaces similar to those that have been used to drive the motion of microliter liquid volumes across surfaces. These methods could also be extended for use as a method of detecting anisotropy in the shape of sessile droplets. Experiments of this kind will be the subject of future studies.

ASSOCIATED CONTENT

Supporting Information

Movie of a vibrating droplet that was collected using a Genie HC640 camera (Teledyne DALSA) at 200 fps. This material is available free of charge via the Internet at http://pubs.acs.org.

AUTHOR INFORMATION

Corresponding Author

*Telephone: +44-(0)115-9515142. Fax: +44-(0)115-9515180. E-mail: james.sharp@nottingham.ac.uk.

Notes

The authors declare no competing financial interest.

ACKNOWLEDGMENTS

The authors thank the Engineering and Physical Sciences Research Council, U.K., for funding under Grant EP/H004939/1.

REFERENCES

(1) Langley, K. R.; Sharp, J. S. Microtextured surfaces with gradient wetting properties. *Langmuir* **2010**, *26*, 18349−18356.
(2) Noblin, X.; Kofman, R.; Celestini, F. Rachetlike motion of a shaken drop. *Phys. Rev. Lett.* **2009**, *102*, 194504.
(3) Brunet, P.; Eggers, J.; Deegan, R. Vibration-induced climbing drops. *Phys. Rev. Lett.* **2007**, *99*, 144501.
(4) Shastry, A.; Case, M. J.; Bohringer, K. Directing droplets using microstructured surfaces. *Langmuir* **2006**, *22*, 6161−6167.
(5) Daniel, S.; Sircar, S.; Gliem, J.; Chaudhury, M. Ratcheting motion of liquid drops on gradient surfaces. *Langmuir* **2004**, *20*, 4085−4092.
(6) Daniel, S.; Chaudhury, M. K.; de Gennes, P.-G. Vibration-actuated drop motion on surfaces for batch microfluidic processes. *Langmuir* **2005**, *21*, 4240−4248.
(7) Tsamopoulos, J. A.; Brown, R. A. Nonlinear oscillations of inviscid drops and bubbles. *J. Fluid Mech.* **1983**, *127*, 519−537.
(8) Lundgren, T. S.; Mansour, N. N. Oscillations of drops in zero gravity with weak viscous effects. *J. Fluid Mech.* **1988**, *194*, 479−510.
(9) Basaran, O. Nonlinear oscillations of viscous liquid drops. *J. Fluid Mech.* **1992**, *241*, 169−198.
(10) James, A. J.; Vukasinovic, B.; Smith, M. K.; Glezer, A. Vibration-induced drop atomization and bursting. *J. Fluid Mech.* **2003**, *476*, 1−28.
(11) Vukasinovic, B.; Smith, M. K.; Glezer, A. Dynamics of a sessile drop in forced vibration. *J. Fluid Mech.* **2007**, *587*, 395−423.
(12) Pan, C. T.; Shiea, J.; Shen, S. C. Fabrication of an integrated piezo-electric micro-nebulizer for biochemical sample analysis. *J. Micromech. Microeng* **2007**, *17*, 659−669.
(13) Wang, P.; Maheshwari, S.; Chang, H. C. Polyhedra formation and transient cone ejection of a resonant microdrop forced by an ac electric field. *Phys. Rev. Lett.* **2006**, *96*, 254502.
(14) Mugele, F.; Baret, J.-C.; Steinhauser, D. Microfluidic mixing through electrowetting-induced droplet oscillations. *App. Phys. Lett.* **2006**, *88*, 204106.
(15) Hansen, F. Surface tension by image analysis: fast and automatic measurements of pendant and sessile drops and bubbles. *J. Colloid Interface Sci.* **1993**, *160*, 209−217.
(16) Sharp, J. S.; Farmer, D. J.; Kelly, J. Contact angle dependence of the resonant frequency of sessile water droplets. *Langmuir* **2011**, *27*, 9367−9371.
(17) Hill, R.; Eaves, L. Vibrations of a diamagnetically levitated water droplet. *Phys. Rev. E* **2010**, *81*, 1−8.
(18) Sharp, J. S. Resonant properties of sessile droplets; contact angle dependence of the resonant frequency and width in glycerol/water mixtures. *Soft Matter* **2012**, *8*, 399−407.
(19) Bastrukov, S. I. Elastodynamics of self-gravitating matter: Nonradial vibrations of a star modeled by a heavy spherical mass of an elastic solid. *Phys. Rev. E* **1996**, *53*, 1917.
(20) Abul-Magd, A. Y.; Simbel, M. H. Analytical calculation of fusion barrier distributions. *Phys. Rev. C* **1998**, *58*, 2229.
(21) Chen, X.; Ma, R.; Li, J.; Hao, C.; Guo, W.; Luk, B. L.; Li, S. C.; Yao, S.; Wang, Z. Evaporation of droplets on superhydrophobic surfaces: Surface roughness and small droplet size effects. *Phys. Rev. Lett.* **2012**, *109*, 116101.
(22) McHale, G.; Brown, C. V.; Newton, M. I.; Wells, G. G.; Sampara, N. Dielectrowetting driven spreading of droplets. *Phys. Rev. Lett.* **2011**, *107*, 186101.
(23) McHale, G.; Shirtcliffe, N. J.; Aqil, S.; Perry, C. C.; Newton, M. I. Topography driven spreading. *Phys. Rev. Lett.* **2004**, *93*, 036102.
(24) Delmas, M.; Monthioux, M.; Ondarcuhu, M. Contact angle hysteresis at the nanometer scale. *Phys. Rev. Lett.* **2011**, *106*, 136102.
(25) Kusumaatmaja, H.; Vrancken, R. J.; Bastiaansen, C. W. M.; Yeomans, J. M. Anisotropic drop morphologies on corrugated surfaces. *Langmuir* **2008**, *24*, 7299−308.
(26) Chen, Y.; He, B.; Lee, J.; Patankar, N. A. Anisotropy in the wetting of rough surfaces. *J. Colloid Interface Sci.* **2005**, *281*, 458−464.
(27) Noblin, X.; Buguin, A.; Brochard-Wyart, F. Vibrations of sessile drops. *Eur. Phys. J.: Spec. Top.* **2009**, *166*, 7−10.
(28) Noblin, X.; Buguin, A.; Brochard-Wyart, F. Vibrated sessile drops: Transition between pinned and mobile contact line oscillations. *Eur. Phys. J. E: Soft Matter Biol. Phys.* **2004**, *14*, 395−404.
(29) Karadag, Y.; Jonas, A.; Tasaltin, N.; Kiraz, A. Determination of microdroplet contact angles using electrically driven droplet oscillations. *App. Phys. Lett.* **2011**, *98*, 194101.
(30) Mettu, S.; Chaudhury, M. K. Resonance modes of the surface and the slipping contact line of a sessile liquid drop subjected to random vibration. *Langmuir* **2012**, *28*, 14100−14106.
(31) Rayleigh, L. On the capillary phenomena of jets. *Proc. R. Soc. London* **1879**, *29*, 71−97.
(32) Lamb, H. *Hydrodynamics*, 6th ed.; Cambridge University Press: Cambridge, U.K., 1879; pp 639−642.
(33) Chandrasekhar, S. The oscillations of a viscous liquid globe. *Proc. London Math. Soc.* **1959**, *s3−s9*, 141−149.
(34) Strani, M.; Sabetta, F. Free vibrations of a drop in partial contact with a solid support. *J. Fluid Mech.* **1984**, *141*, 233−247.
(35) Strani, M.; Sabetta, F. Viscous oscillations of a supported drop in an immiscible fluid. *J. Fluid Mech.* **1988**, *189*, 397−421.
(36) Wilkes, E. D.; Basaran, O. A. Forced oscillations of pendant (sessile) drops. *Phys. Fluids* **1997**, *9*, 1512−1528.
(37) Celestini, F.; Kofman, R. Vibration of submillimeter-size supported droplets. *Phys. Rev. E* **2006**, *73*, 041602.
(38) Lyubimov, D. V.; Lyubimova, T. P.; Shklyaev, S. V. Behavior of a drop on an oscillating solid plate. *Phys. Fluids* **2006**, *18*, 012101.

(39) Bostwick, J. B.; Steen, P. H. Capillary oscillations of a constrained liquid drop. *Phys. Fluids* **2009**, *21*, 032108.
(40) Prosperetti, A. Linear oscillations of constrained drops, bubbles, and plane liquid surfaces. *Phys. Fluids* **2012**, *24*, 032109.
(41) Ramalingam, S.; Ramkrishna, D.; Basaran, O. A. Free vibrations of a spherical drop constrained at an azimuth. *Phys. Fluids* **2012**, *24*, 082102.
(42) Landau, L. D.; Lifschitz, E. M. *Fluid Mechanics*, 2nd ed.; Pergamon Press: Oxford, U.K., 1987; Chapter 7, pp 238−250.
(43) Webster, J. G. *The Measurement, Instrumentation and Sensors Handbook*; Springer: New York, 1999; Chapter 31
(44) Tadmor, R. Line energy and the relation between advancing, receding, and young contact angles. *Langmuir* **2004**, *20*, 7659−7664.
(45) Ruiz-Cabello, F. J. M.; Rodrguez-Valverde, M. A.; Cabrerizo-Vlchez, M. A. Comparison of the relaxation of sessile drops driven by harmonic and stochastic mechanical excitations. *Langmuir* **2011**, *27*, 8748−8752.
(46) Chaudhury, M. K.; Whitesides, G. M. How to make water run uphill. *Science* **1992**, *256*, 1539−1541.
(47) Cummings, D. L.; Blackburn, D. A. Oscillations of magnetically levitated aspherical droplets. *J. Fluid Mech.* **1991**, *224*, 395−416.
(48) Lide, D.; Weast, R. *CRC Handbook of Chemistry and Physics*, 69th ed.; CRC Press: Boca Raton, FL, 1888; pp F10−F34.